Compensating losses in negative-index metamaterials by optical parametric amplification

Alexander K. Popov

Department of Physics and Astronomy and Department of Chemistry, University of Wisconsin–Stevens Point, Stevens Point, Wisconsin 54481-3897

Vladimir M. Shalaev

School of Electrical and Computer Engineering, Purdue University, West Lafayette, Indiana 47907-2035

Optical parametric amplification controlled by the auxiliary electromagnetic field enables transparency, amplification, and oscillation with no cavity in strongly absorbing negative-index metamaterials. The opposite directions of the wave vector and the Poynting vector in such materials result in extraordinary optical properties, including "backward" phase matching and the generation of entangled pairs of left- and right-handed counterpropagating photons. © 2006 Optical Society of America

OCIS code: 190.4410.

Metamaterials with a negative refractive index (NIMs), also referred to as left-handed metamaterials (LHMs), exhibit highly unusual electromagnetic properties and promise a variety of novel applications, particularly for nonlinear optical phenomena. As shown recently, NIMs that include structural elements with nonsymmetric current-voltage characteristics can possess a nonlinear magnetic response at optical frequencies[1–3] and thus combine unprecedented linear and nonlinear electromagnetic properties. The opposite directions of the wave and Poynting vectors inherent for NIMs lead to extraordinary properties for basic optical processes in such metamaterials. The possibility of exact phase matching for waves with counterpropagating energy flows has been shown in Ref. 4 for the case of second-harmonic generation (SHG), when the fundamental wave is in the negative-index frequency domain while the SH wave is in the positive-index domain (PID). As seen from our considerations, phase matching of forward and backward waves is inherent for the nonlinear optics of NIMs. Important advantages of the interaction schemes involving counterdirected Poynting vectors in the process of optical parametric amplification for conventional right-handed materials (RHMs), also referred to as positive-index materials (PIMs), were discussed in early papers.[5–7] However, in RHMs such schemes impose severe limitations on the frequencies of the coupled waves, because one of the waves must be in the far-infrared range in this case.[5–7]

Absorption is one of the largest problems that needs to be addressed to enable applications of NIMs.[8,9] A transfer of the near-field image into the SH frequency domain, where absorption is typically much less, was proposed in Refs. 10 and 11 as a means to overcome dissipative losses and thus enable the NIM-based superlens. This Letter proposes an alternative means for compensating losses, by producing entire transparency amplification, or even lasing without a cavity in NIMs, with the aid of only one control auxiliary electromagnetic field. The underlying physical mechanism is based on optical parametric amplification (OPA), where a positive-index control field enables a loss-balancing OPA for a negative-index signal wave. We also predict the possibility of the generation of entangled pairs of counterpropagating right- and left-handed photons.

We assume a negative-index wave at ω_1 (signal; $n_1 < 0$) has a wave vector $\mathbf{k}_1$, which is directed along the z axis, and an energy flow $\mathbf{S}_1$, which is directed against the z axis [Fig. 1(a)]. The medium is illuminated by a higher-frequency wave traveling along the z axis. The frequency of this radiation is ω_3 and is in a PID ($n_3 > 0$). The two coupled waves with codirected wave vectors $\mathbf{k}_3$ and $\mathbf{k}_1$ generate a difference-frequency idler at $\omega_2 = \omega_3 - \omega_1$, which is in a PID ($n_2 > 0$). The idle wave contributes back into the wave at ω_1 through three-wave mixing (TWM) and thus enables OPA at ω_1 by converting the energy of the pump field at ω_3 into the signal. We note that, all three interacting waves have their wave vectors codirected along z, whereas the energy flow of the signal wave $\mathbf{S}_1$ is directed against z, and thus it is *opposite* to the energy flows of the two other waves $\mathbf{S}_2$ and $\mathbf{S}_3$. Such a coupling scheme is in contrast with the conventional

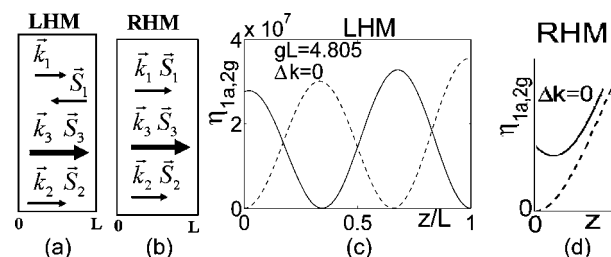Fig. 1. OPA processes in NIMs and PIMs. Phase-matching schemes in (a) LHM and (b) RHM. The phase-matched amplification factor for the signal wave (η_{1a}, solid curve), and the conversion factor for the idler wave (η_{2g}, dashed curve) in (c) LHM and (d) RHM with absorption ($\alpha_1 L = 1$, $\alpha_2 L = 1/2$); (d) represents the dependence schematically.

© 2006 Optical Society of America

phase-matching scheme for OPA in RHMs [Fig. 1(b)]. This, in turn, results in different spatial intensity dependencies in LHMs and RHMs. Figure 1(c) displays the periodical oscillations along a NIM slab even at $\Delta k = 0$, whereas exponential growth for both waves occurs in PIMs at large z [Fig. 1(d)]. The noted results for NIMs are obtained from Eqs. (7) and (8); see below.

Optical magnetization plays a crucial role in NIMs. Following the method in Ref. 4, we assume that the nonlinear response is quadratic and associated with the magnetic component of the waves:

$$H_j(z,t) = h_j \exp[i(k_j z - \omega_j t)] + \text{c.c.} \qquad (1)$$

$(j=1,2,3)$. The nonlinear magnetization at the signal and idler frequencies is given by

$$M_{1,2}^{NL} = 2\chi_{\text{eff}}^{(2)} h_3 h_{2,1}^* \exp\{i[(k_3 - k_{2,1})z - \omega_{1,2}t]\}. \qquad (2)$$

Here $\omega_2 = \omega_3 - \omega_1$, $k_j = |n_j|\omega_j/c > 0$, and $\chi_{\text{eff}}^{(2)}$ is the nonlinear susceptibility. Then, the slowly varying normalized amplitudes $a_j = \sqrt[4]{\epsilon_j/\mu_j} h_j/\sqrt{\omega_j}$ for the signal and idler waves can be written in the form

$$da_1/dz = -iga_2^* \exp(i\Delta kz) + (\alpha_1/2)a_1, \qquad (3)$$

$$da_2/dz = iga_1^* \exp(i\Delta kz) - (\alpha_2/2)a_2, \qquad (4)$$

where $g = (\sqrt{\omega_1\omega_2}/\sqrt[4]{\epsilon_1\epsilon_2/\mu_1\mu_2})(8\pi/c)\chi^{(2)}h_3$, $\Delta k = k_3 - k_2 - k_1$, and α_j are the absorption coefficients. The pump amplitude h_3 is assumed to be constant. The squared values of $a_{1,2}$ are proportional to the number of photons at the corresponding frequencies. We note the asymmetry in Eqs. (3) and (4), which is not the case for PIMs. The asymmetry reflects *three fundamental differences* in Eq. (3) as compared with a conventional difference-frequency generation (DFG) resulting from the TWM of copropagating waves in PIMs. First, the sign for the nonlinear polarization term is opposite to that in Eq. (4), which occurs because $\epsilon_1 < 0$. Second, the opposite sign appears with α_1 because the energy flow $\mathbf{S}_1$ is directed against the z axis. Finally, the boundary conditions for a_1 are defined at the opposite side of the sample, as compared with a_2 and h_3, because the flows $\mathbf{S}_1$ and $\mathbf{S}_2$ are counterdirected. For $\alpha_1 = \alpha_2 = 0$, one finds

$$d[(S_{1z}/\hbar\,\omega_1) - (S_{2z}/\hbar\,\omega_2)]/dz = 0, \qquad (5)$$

$$d[\sqrt{\mu_1/\epsilon_1}(h_1^2/\omega_1) + \sqrt{\mu_2/\epsilon_2}(h_2^2/\omega_2)]/dz = 0. \qquad (6)$$

These equations represent the Manley–Rowe relations, which describe the creation of pairs of entangled counterpropagating photons $\hbar\omega_1$ and $\hbar\omega_2$. Equation (6) accounts for the opposite signs of the corresponding derivatives with respect to z; it predicts that the *sum* of the terms proportional to the squared amplitudes for the signal and idler will remain constant through the sample, which is in contrast with the requirement that the *difference* of such terms be constant in a PIM.

Taking into account the boundary conditions $a_1(L) = a_{1L}$ and $a_2(0) = a_{20}$ (where L is the slab thickness), the solutions to Eqs. (3) and (4) can be written as

$$a_1(z) = A_1 \exp(\beta_1^+ z) + A_2 \exp[(\beta_2^+ z)], \qquad (7)$$

$$a_2^*(z) = \kappa_1 A_1 \exp(\beta_1^- z) + \kappa_2 A_2 \exp(\beta_2^- z), \qquad (8)$$

where

$$\beta_{1,2}^\pm = \beta_{1,2} \pm (i\Delta k/2), \quad \beta_{1,2} = (\alpha_1 - \alpha_2)/(4) \pm iR,$$

$$A_{1,2} = \pm[a_{1L}\kappa_{2,1} - a_{20}^* \exp(\beta_{2,1}^+ L)]/D,$$

$$D = \kappa_2 \exp(\beta_1^+ L) - \kappa_1 \exp(\beta_2^+ L),$$

$$\kappa_{1,2} = (\pm R + is)/g, \quad R = \sqrt{g^2 - s^2},$$

$$s = (\alpha_1 + \alpha_2)/(4) - i(\Delta k/2). \qquad (9)$$

The amplification factor for the negative-index signal wave at $a_{20} = 0$ is given by $\eta_{1a}(z) = |a_1(z)/a_{1L}|^2$. The corresponding conversion factor for the positive-index idler resulting from DFG is given by $\eta_{2g}(z) = |a_2(z)^*/a_{1L}|^2$. Note that, a negative-index wave can be generated even when $a_{1L} = 0$; then the conversion factor for the signal is given by $\eta_{1g}(z) = |a_1(z)/a_{20}^*|^2$.

Equations (7) and (8) predict unusual properties for the TWM process in a NIM, which are in sharp contrast with those in PIMs. Figures 2(a) and 2(b) show the oscillatory behavior of the amplification factor η_{1a} and the conversion efficiency for the idler η_{2g} at relatively large intensities of the control field $gL = 14.17$ for both $\Delta k = 0$ and $\Delta k = \pi$. Note that, in contrast to PIMs, the oscillations occur even at $\Delta k = 0$ [see also Fig. 1(c)]. This unusual behavior takes place because the signal and idler increase in opposite directions, and they are determined by the boundary conditions on the opposite sides of a NIM slab. As a result, the amplification threshold in NIMs appears for the product gL rather than for g as in PIMs. Figures 2(a) and 2(b) and 2(c)–2(e) also show strong dependence of amplification and the DFG efficiency on the phase matching for both larger ($gL = 14.17$) and smaller ($gL = 1.82$) magnitudes of the control field.

The comparison of Fig. 2(f) with Fig. 2(c) ($\Delta k = 0$ in both figures) shows a strong resonance dependence of the DFG efficiency in NIMs on the parameter gL, indicating the necessity of fine tuning for the intensity of the control field. According to these figures, unless the pump intensity and phase matching are appropriately optimized, the maximum for the negative-index signal may occur inside rather than at the output edge of the sample.

We also note that Figs. 2(a), 2(b), and 1(c) illustrate the generation of pairs of entangled right- and left-handed photons propagating in opposite directions.

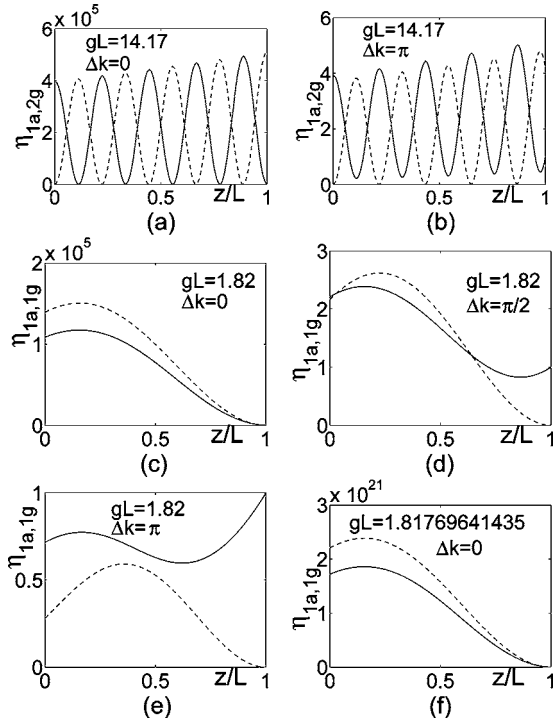At $a_{20} = 0$, the output value of a_{10} is given by

Fig. 2. Amplification factor for the negative-index signal [$\eta_{1a}(z) = |a_1/a_{1L}|^2$; solid curves in (a)–(f)], the conversion factor for the signal [$\eta_{1g}(z) = |a_1/a_{20}^*|^2$; dashed curves in (c)–(f)]; and the conversion factor for the positive-index idler [$\eta_{2g}(z)|a_2/a_{1L}^*|^2$; dashed curves in (a) and (b)] for various Δk and gL. $\alpha_1 L = 1$, $\alpha_2 L = 1/2$.
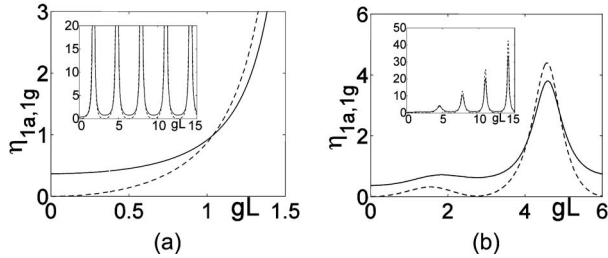

Fig. 3. Output amplification, η_{1a} (solid curve), and DFG conversion factor, η_{1g} (dashed curve) for the backward wave at $z = 0$. (a) $\Delta k = 0$. (b) $\Delta kL = \pi$. Insets, sets of periodical resonances for $\eta_{1a,1g}$ versus gL. $\alpha_1 L = 1$, $\alpha_2 L = 1/2$.

$$\frac{a_1(z=0)}{a_{1L}} = \frac{\exp\left[-\left(\frac{\alpha_1 - \alpha_2}{4} + i\frac{\Delta k}{2}\right)L\right]}{\cos RL + \left(\frac{\alpha_1 + \alpha_2}{4R} - i\frac{\Delta k}{2R}\right)\sin RL}.$$

(10)

Alternatively, at $a_{1L} = 0$, it is given by

$$\frac{a_1(z=0)}{a_{20}^*} = \frac{-(g/R)\sin RL}{\cos RL + \left(\frac{\alpha_1 + \alpha_2}{4R} - i\frac{\Delta k}{2R}\right)\sin RL}.$$

(11)

Equations (10) and (11) show that the output magnitude of the negative-index wave tends to infinity

when the denominator approaches zero. This indicates the possibility of an oscillation with no cavity. For physics of cavityless oscillation, see Ref. 7.

Figure 3 illustrates such resonance dependence on the intensity of the control field at ω_3 (via the gL parameter) for $\Delta k = 0$ [Fig. 3(a)] and $\Delta k = \pi$ [Fig. 3(b)]. Figures 2 and 3 both show that the amplification for a phase-matched wave can reach many orders of magnitude in the maximums. Such OPA can not only compensate for absorption but even turn into optical parametric oscillations (OPOs) when the intensity of the control field reaches specific values given by a periodic set of the increasing numbers. The important advantage of the backward OPA and OPO in NIMs is distributed feedback, which enables oscillations without a cavity. In NIMs, each spatial point serves as a source for the generated wave in the reflected direction, whereas the phase velocities of all the three coupled waves are codirected.

In conclusion, we showed the feasibility of compensating losses in negative-index materials (NIMs) by OPA. In this process, the wave vectors of all three coupled waves are codirected, whereas the energy flow for the signal negative-index wave is counterdirected with respect to those for the pump and the idler waves. This process is characterized by properties that are in sharp contrast with those known for conventional nonlinear optical media. The possibility of OPOs without a cavity at frequencies where the refractive index is negative is also shown. Finally, OPA and OPO in NIMs enable the generation of pairs of entangled counterpropagating right- and left-handed photons.

References

1. M. Lapine, M. Gorkunov, and K. H. Ringhofer, Phys. Rev. E **67**, 065601 (2003).
2. A. A. Zharov, I. V. Shadrivov, and Yu. S. Kivshar, Phys. Rev. Lett. **91**, 037401 (2003).
3. M. Lapine and M. Gorkunov, Phys. Rev. E **70**, 66601 (2004).
4. I. V. Shadrivov, A. A. Zharov, and Yu. S. Kivshar, arXiv.org, http://arxiv.org/abs/physics/0506092.
5. S. E. Harris, Appl. Phys. Lett. **9**, 114 (1966).
6. K. I. Volyak and A. S. Gorshkov, Radiotekh. Elektron. (Moscow) **18**, 2075 (1973) (in Russian).
7. A. Yariv, *Quantum Electronics*, 2nd ed. (Wiley, 1975), Sec. 17.8.
8. K. J. Webb, M. Yang, D. W. Ward, and K. A. Nelson, Phys. Rev. E **70**, 035602R (2004).
9. V. A. Podolskiy, N. A. Kuhta, and G. W. Milton, Appl. Phys. Lett. **87**, 231113 (2005).
10. V. M. Agranovich, Y. R. Shen, R. H. Baughman, and A. A. Zakhidov, Phys. Rev. B **69**, 165112 (2004).
11. A. A. Zharov, N. A. Zharova, I. V. Shadrivov, and Yu. S. Kivshar, Appl. Phys. Lett. **87**, 091104-3 (2005).